Supporting Information for

Structure-property investigations of benzoylspirocyclic aromatics as small molecule hosts for solution-processable TADF devices

Xiang-Hua Zhao,* Qing-Chun Sun, Ming-Rui Tian, Guohua Xie,* Mu-xin Chen, Qian-qian Chen, Guo-Dong Zou, Bing-Ran Ye, Chu-Yin Meng, Ling-Hai Xie*

Contents:

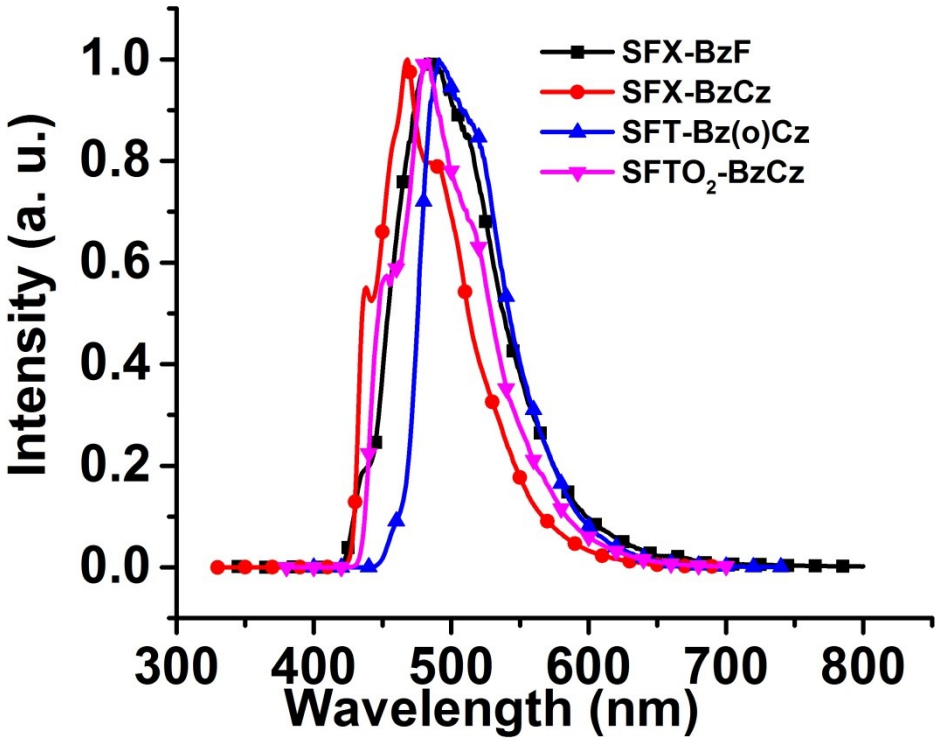

Fig. S1 Phosphorescence spectra of **SFX-BzF, SFX-BzCz, SFT-Bz(o)Cz** and **$SFTO_2$-BzCz** measured at 77 K in CH_2Cl_2

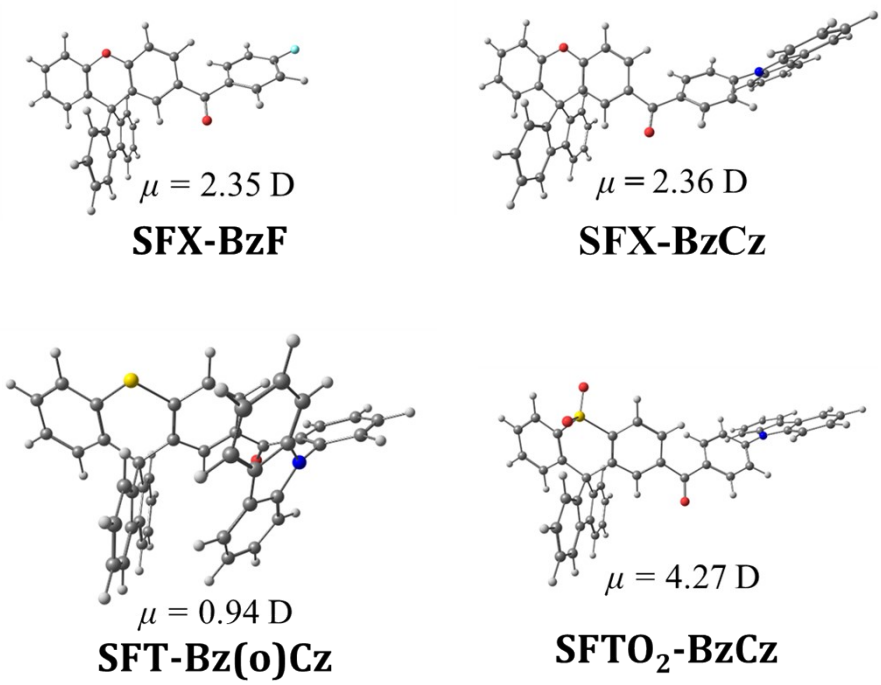

Fig. S2 The polarities of the four hosts calculated by DFT calculations

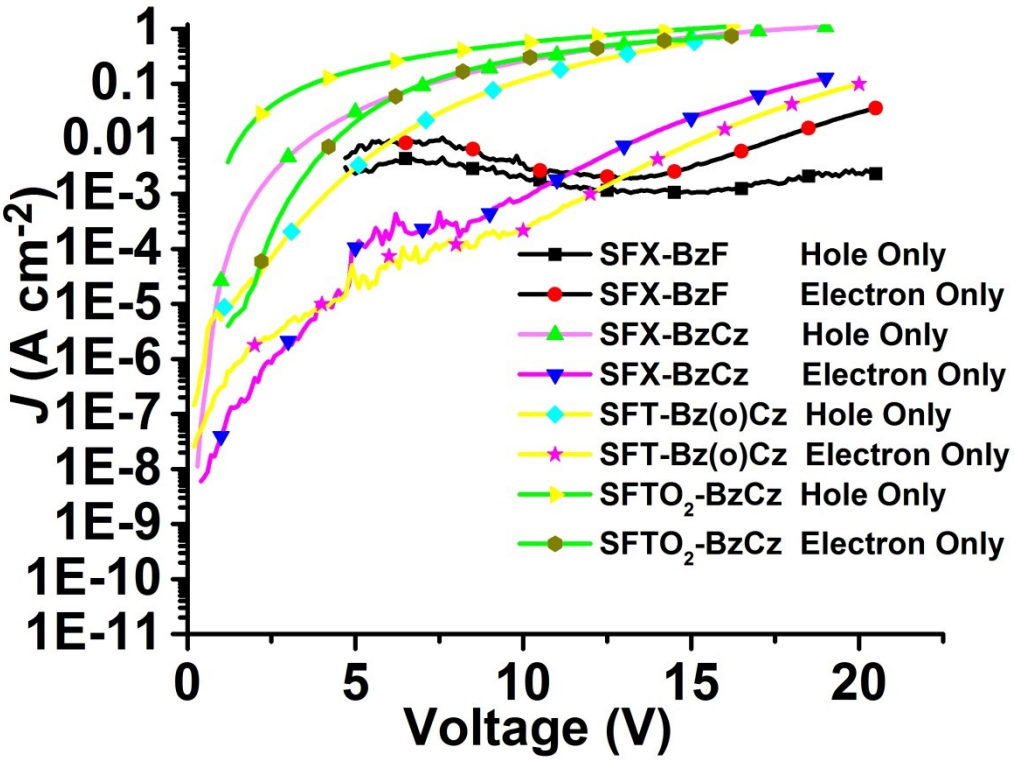

Fig. S3 Current density of hole-only and electron-only devices

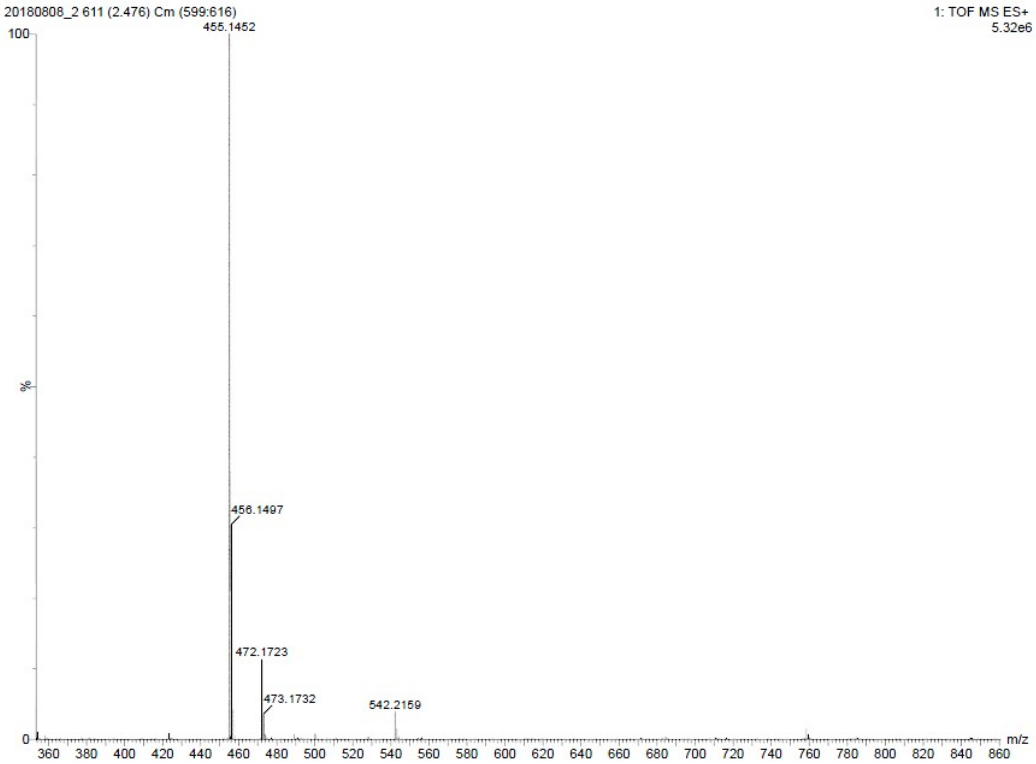

Fig. S4 The LC-MS of **SFX-BzF**

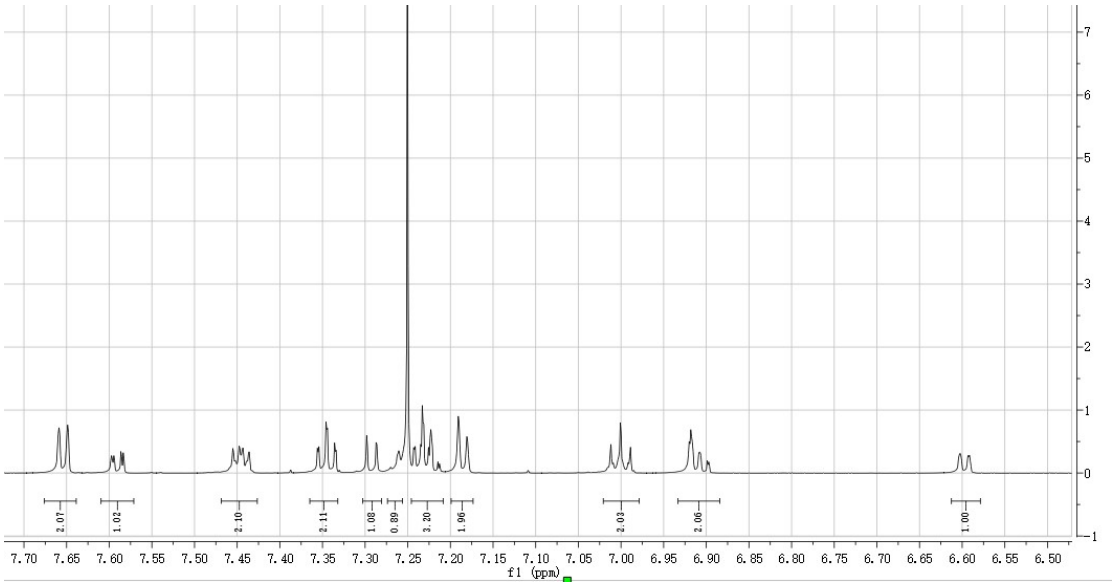

Fig. S5 ^{1}H NMR of **SFX-BzF** in $CDCl_3$

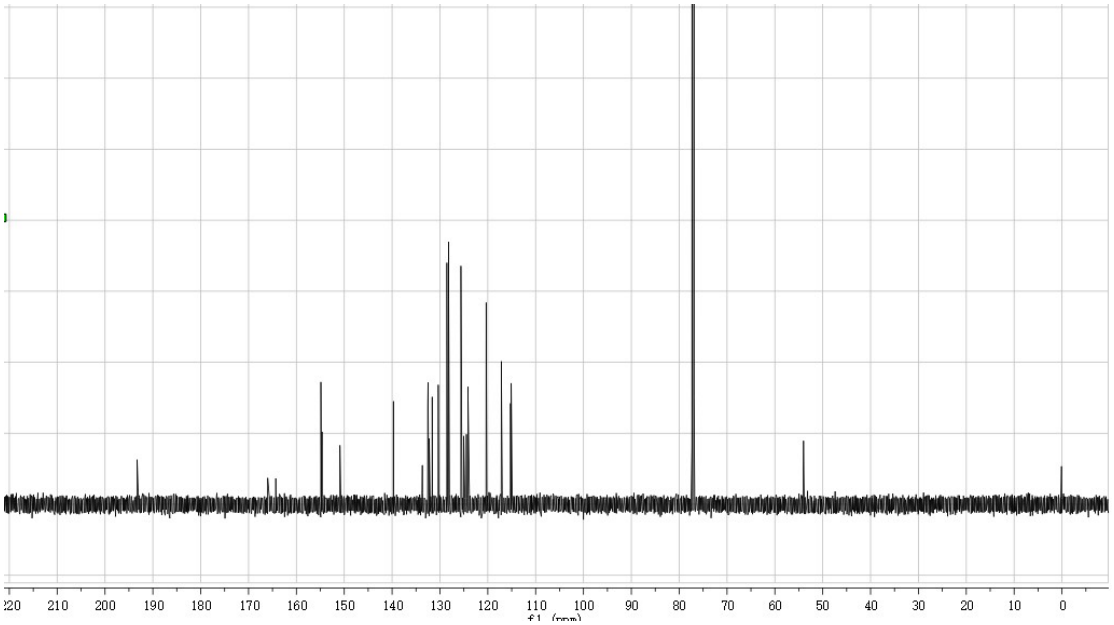

Fig. S6 ^{13}C NMR of **SFX-BzF** in $CDCl_3$

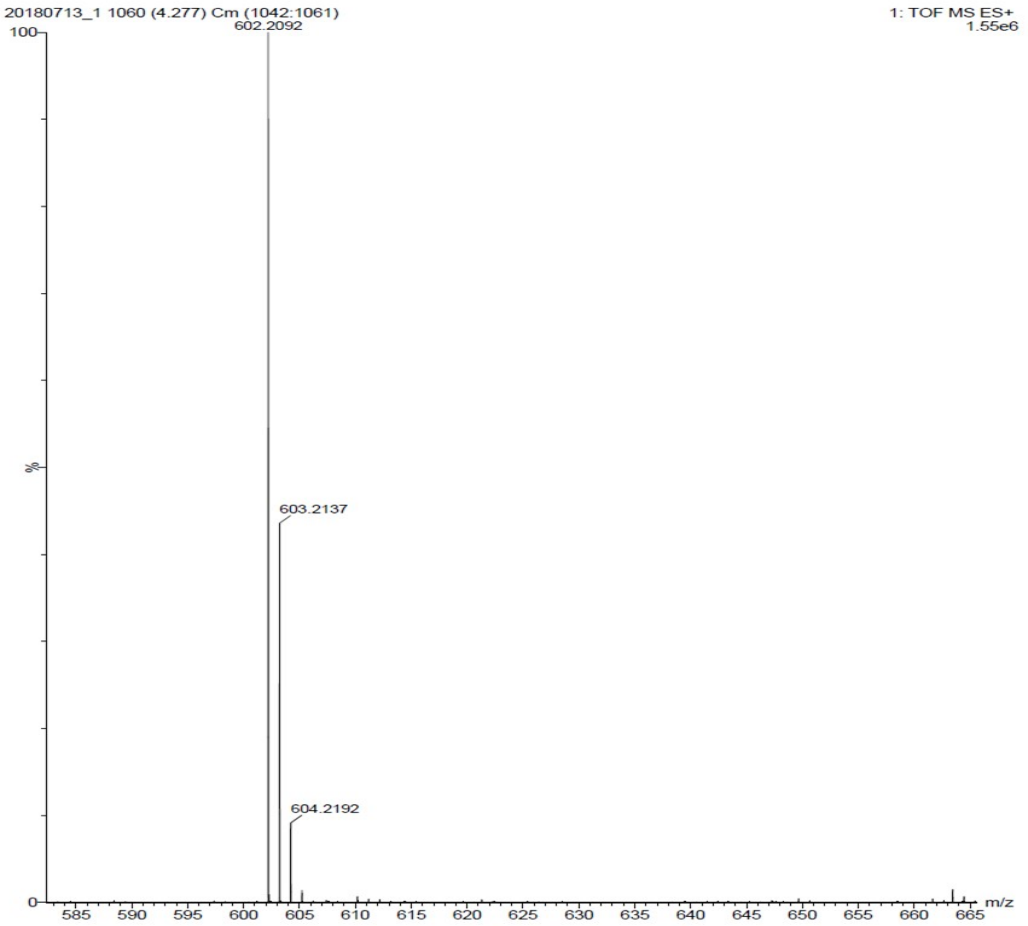

Fig. S7 The LC-MS of **SFX-BzCz**

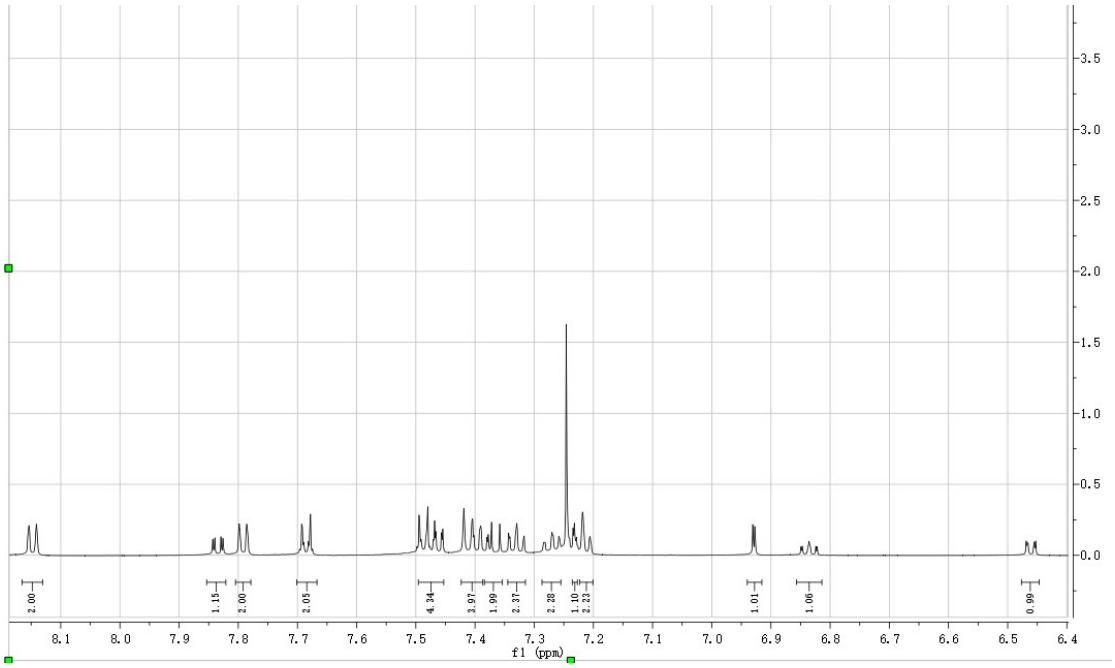

Fig. S8 ^{1}H NMR of **SFX-BzCz** in $CDCl_3$

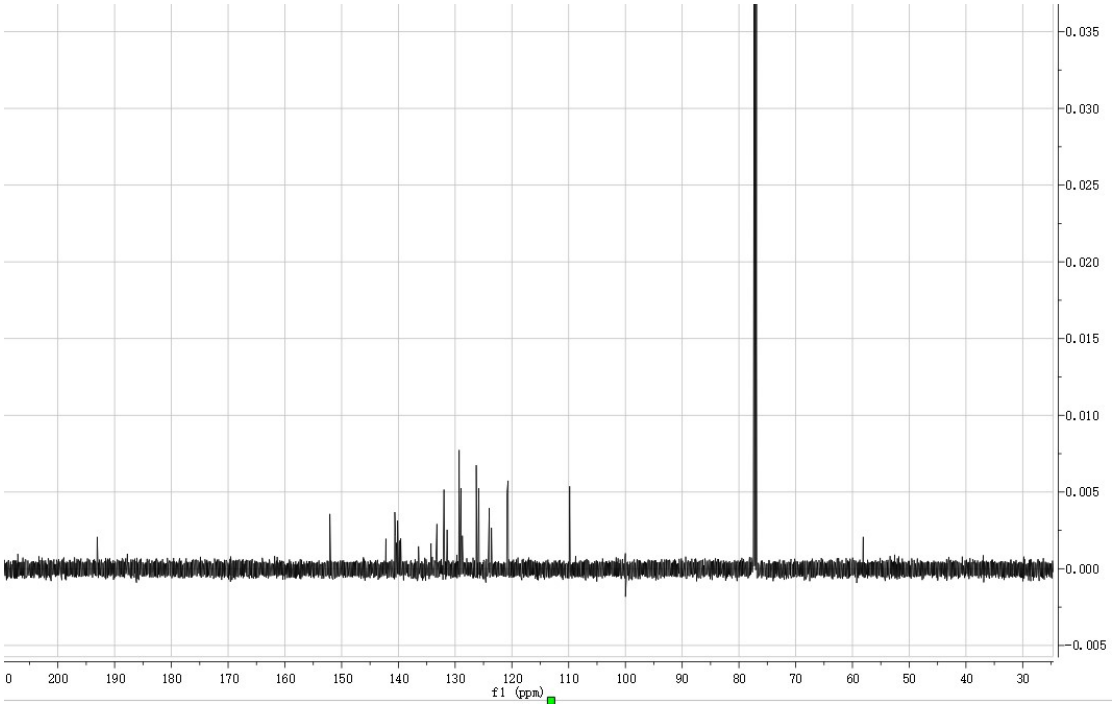

Fig. S9 ^{13}C NMR of **SFX-BzCz** in $CDCl_3$

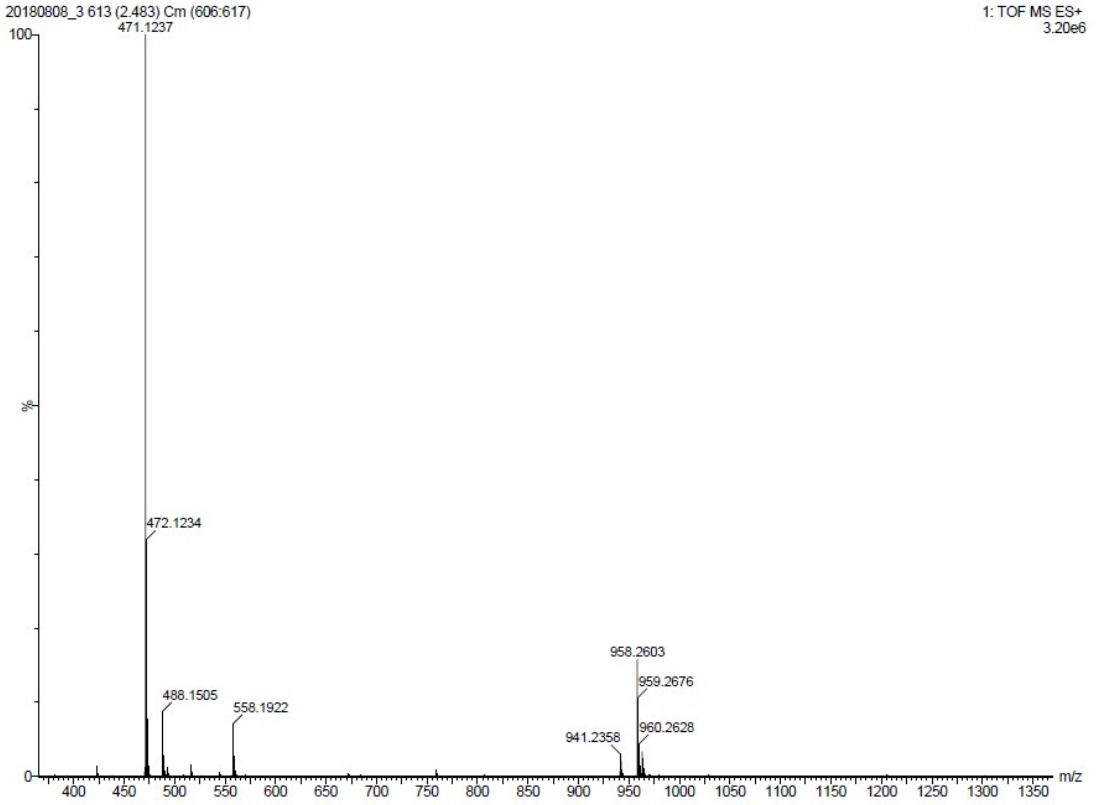

Fig. S10 The LC-MS of **SFT-Bz(o)F**

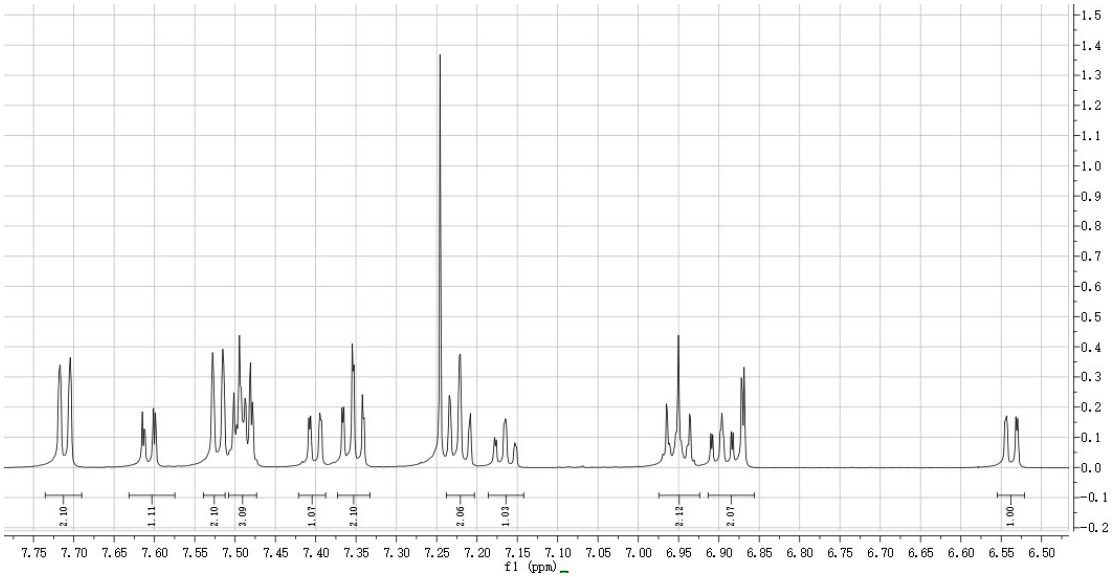

Fig. S11 ^{1}H NMR of **SFT-Bz(o)F** in $CDCl_3$

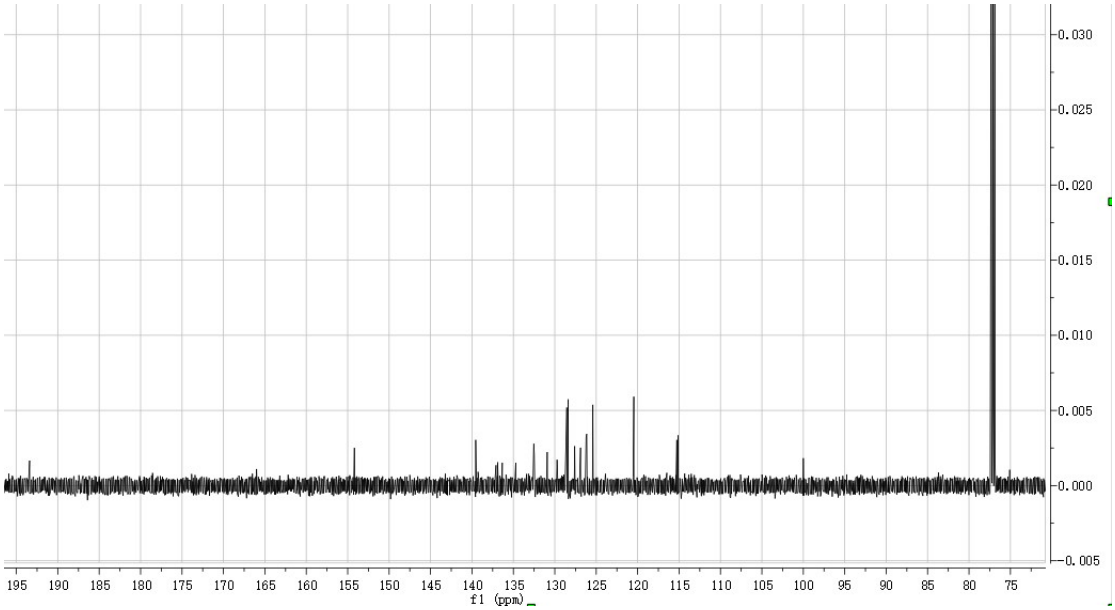

Fig. S12 ^{13}C NMR of **SFT-Bz(o)F** in $CDCl_3$

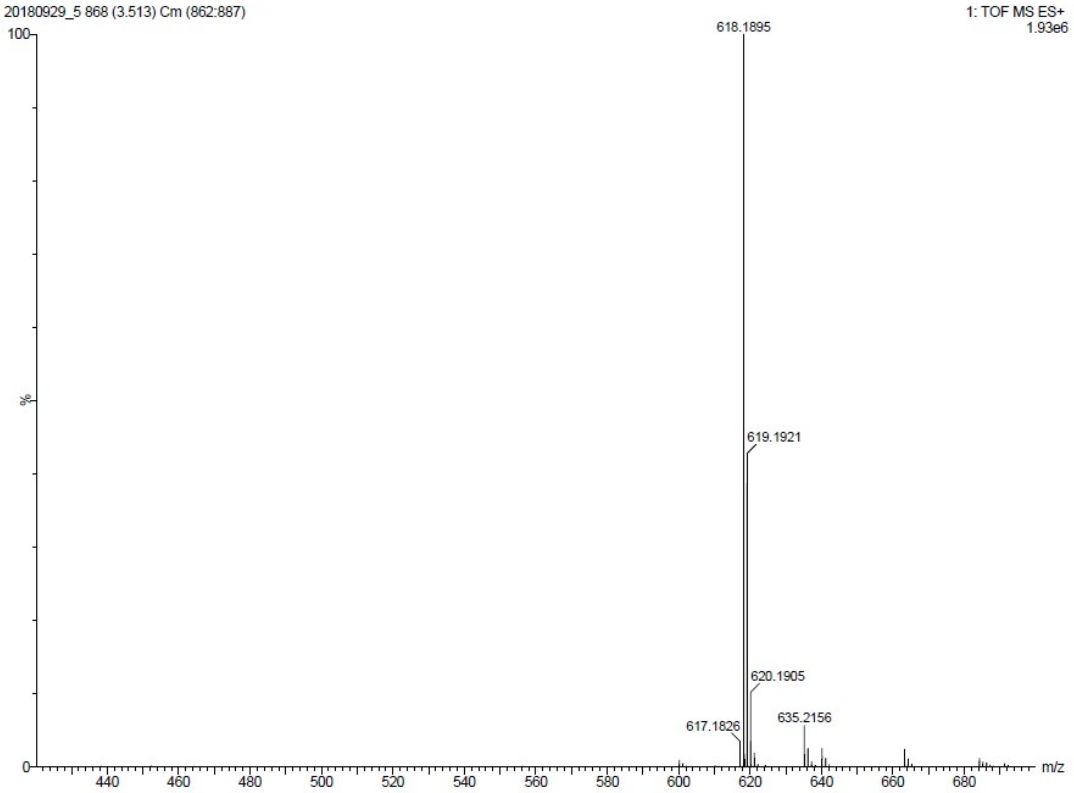

Fig. S13 The LC-MS of **SFT-Bz(o)Cz**

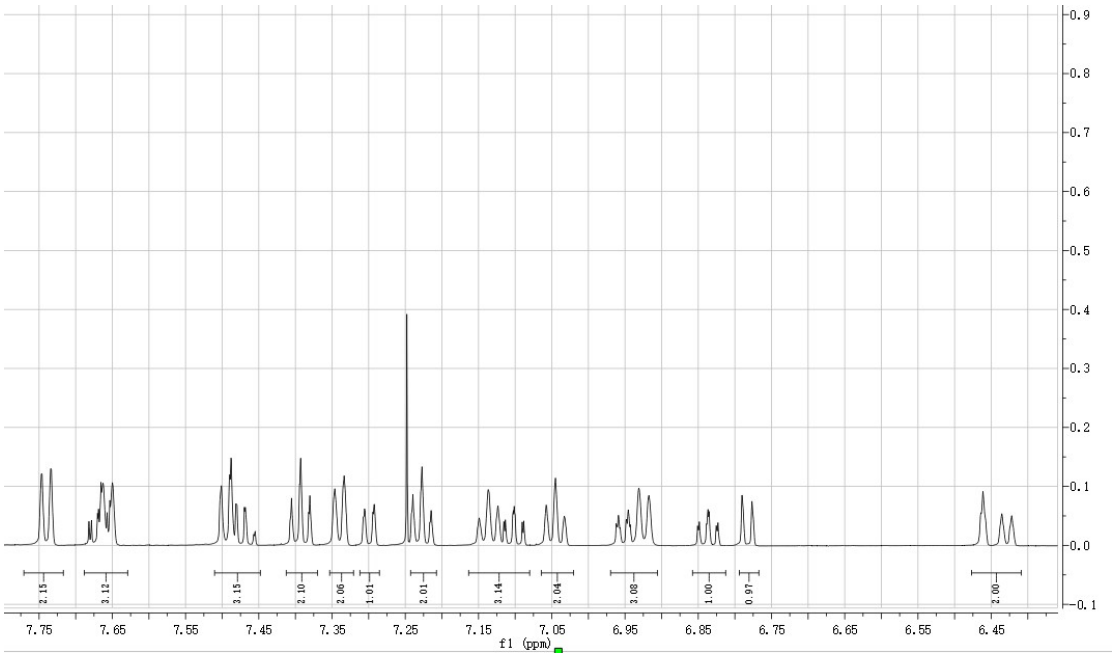

Fig. S14 ^{1}H NMR of **SFT-Bz(o)Cz** in $CDCl_3$

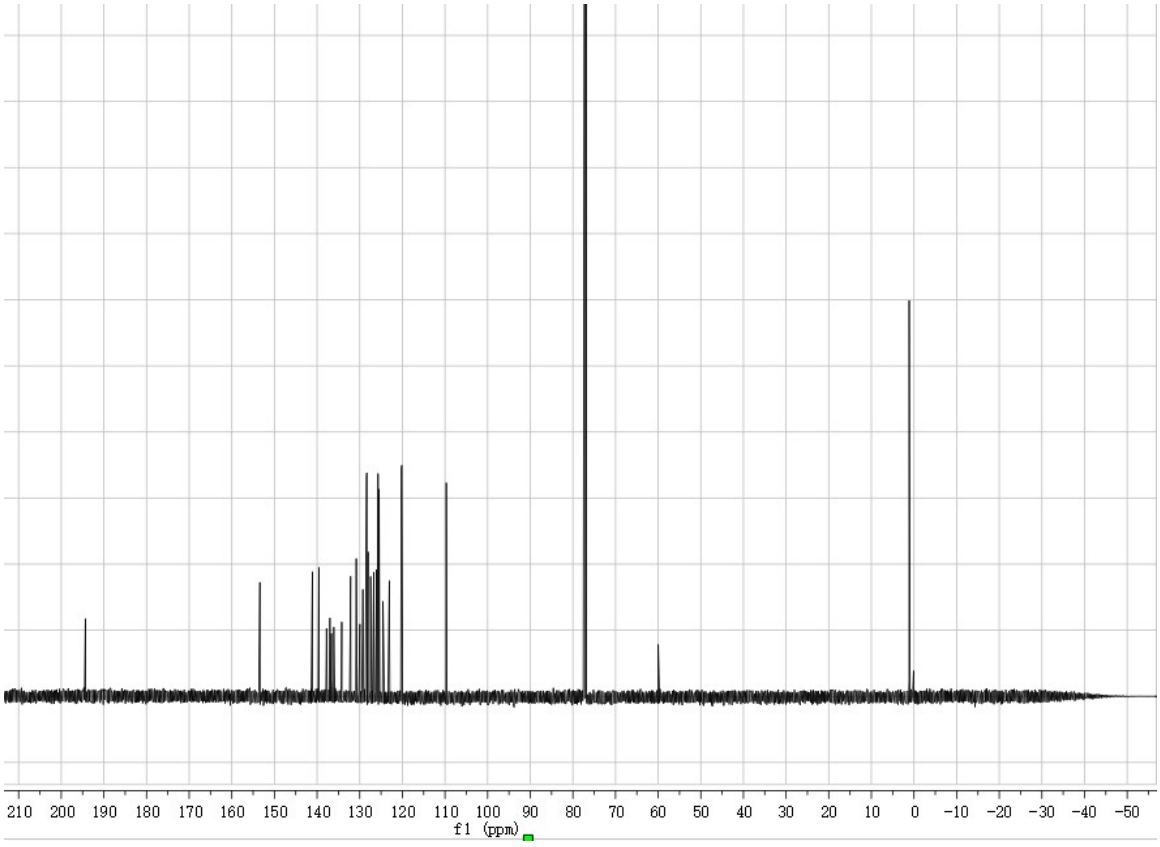

Fig. S15 ^{13}C NMR of **SFT-Bz(o)Cz** in $CDCl_3$

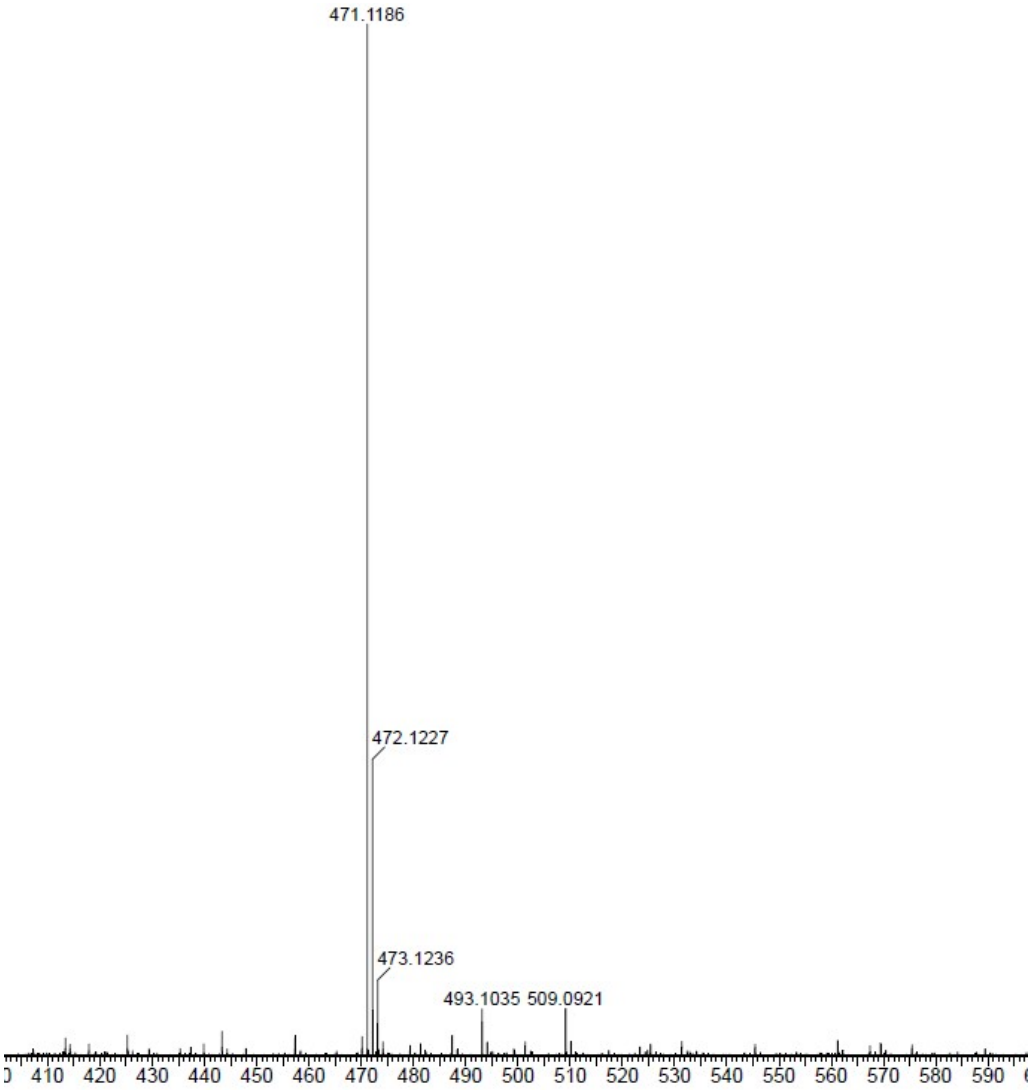

Fig. S16 The LC-MS of **SFT-BzF**

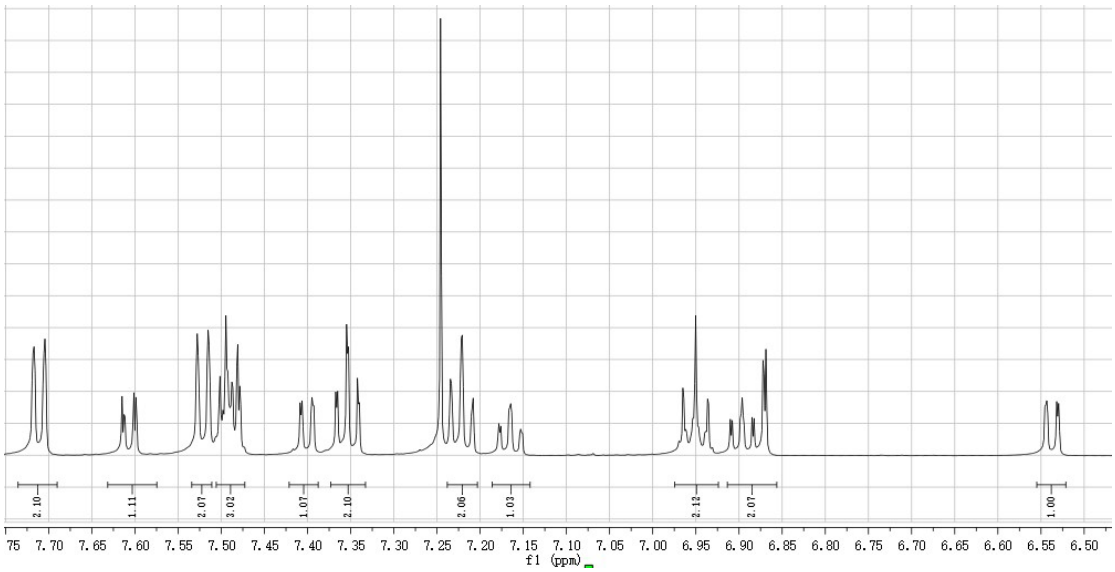

Fig. S17 ^{1}H NMR of **SFT-BzF** in $CDCl_3$

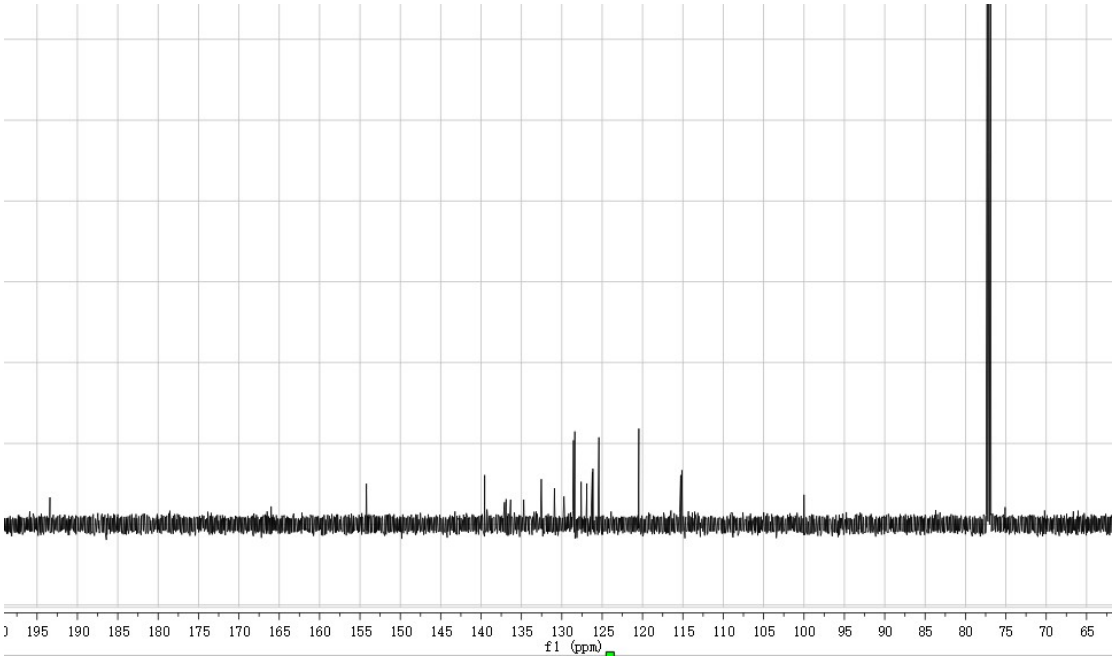

Fig. S18 ^{13}C NMR of **SFT-BzF** in $CDCl_3$

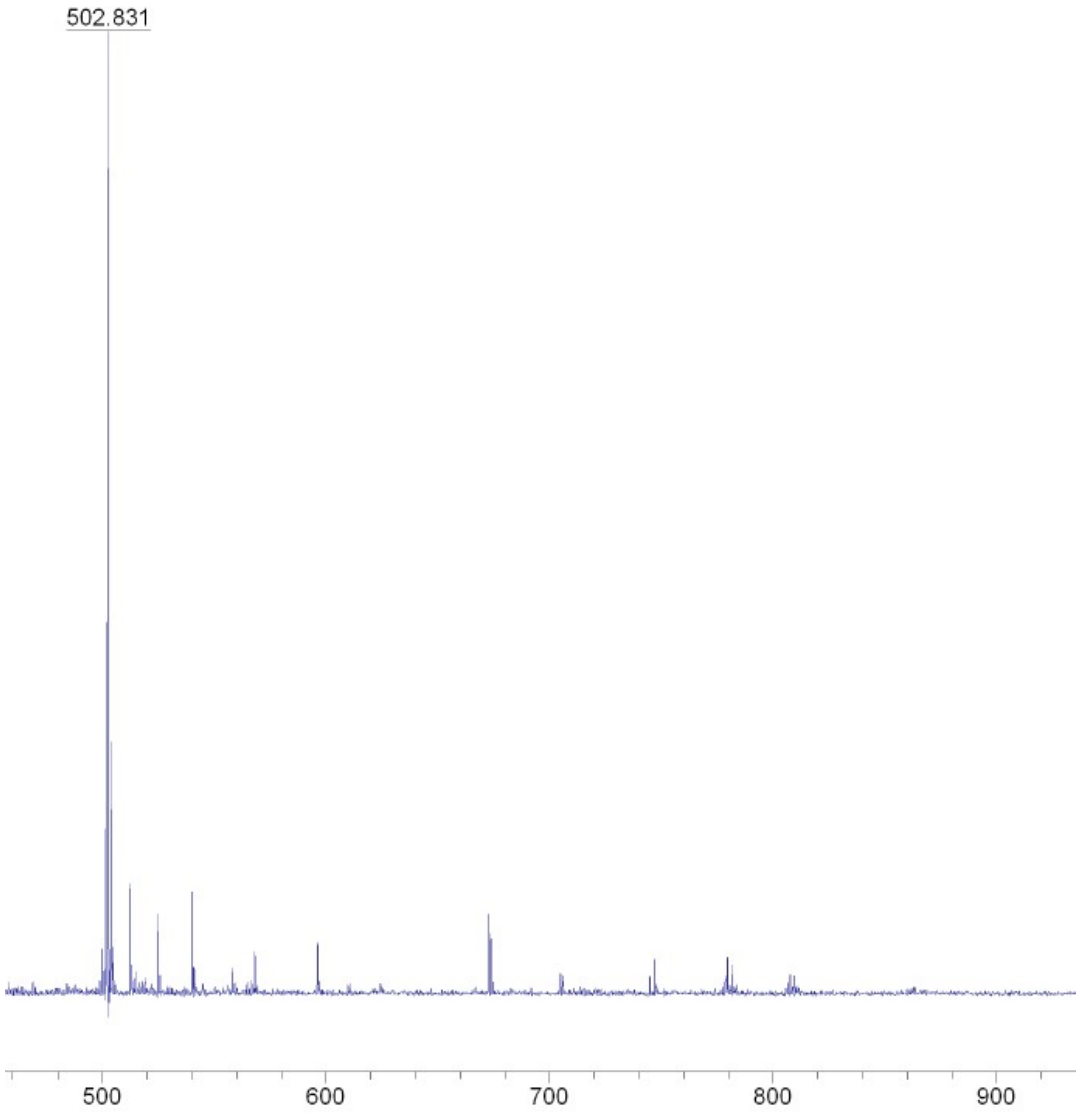

Fig. S19 The LC-MS of **SFTO$_2$-BzF**

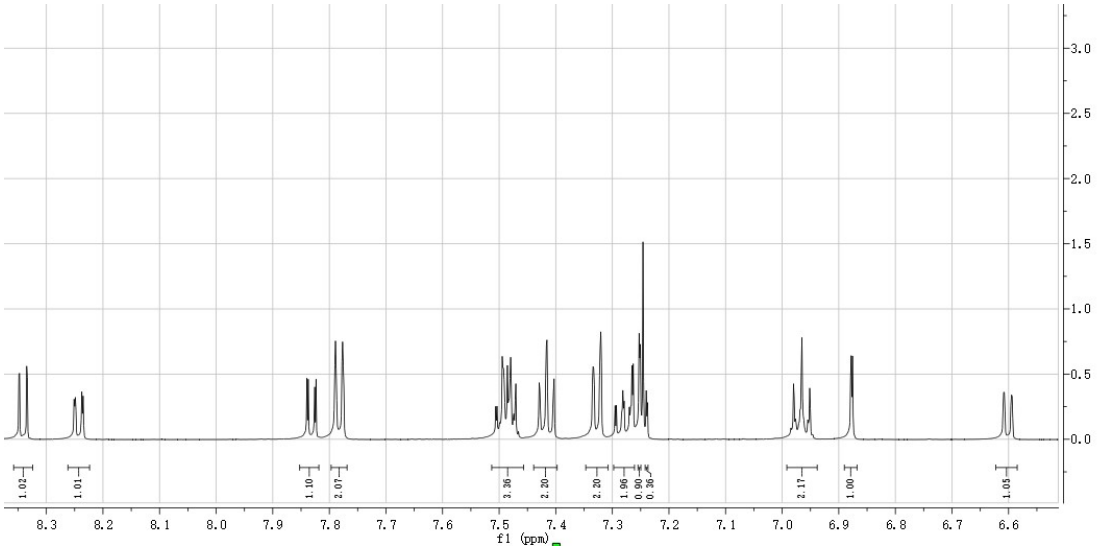

Fig. S20 ^{1}H NMR of **SFTO$_2$-BzF** in $CDCl_3$

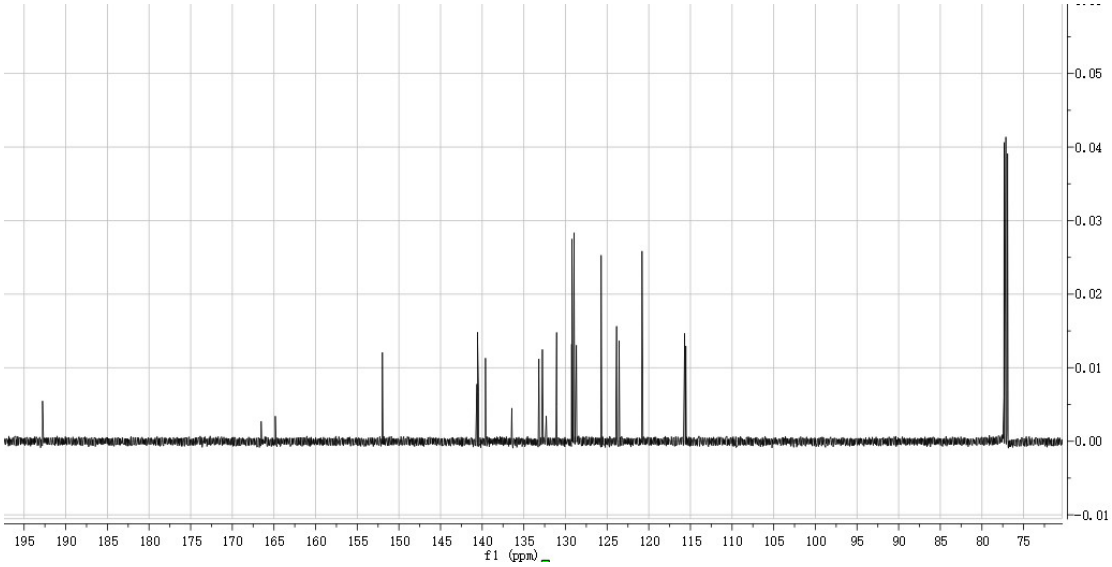

Fig. S21 ^{13}C NMR of **SFTO$_2$-BzF** in $CDCl_3$

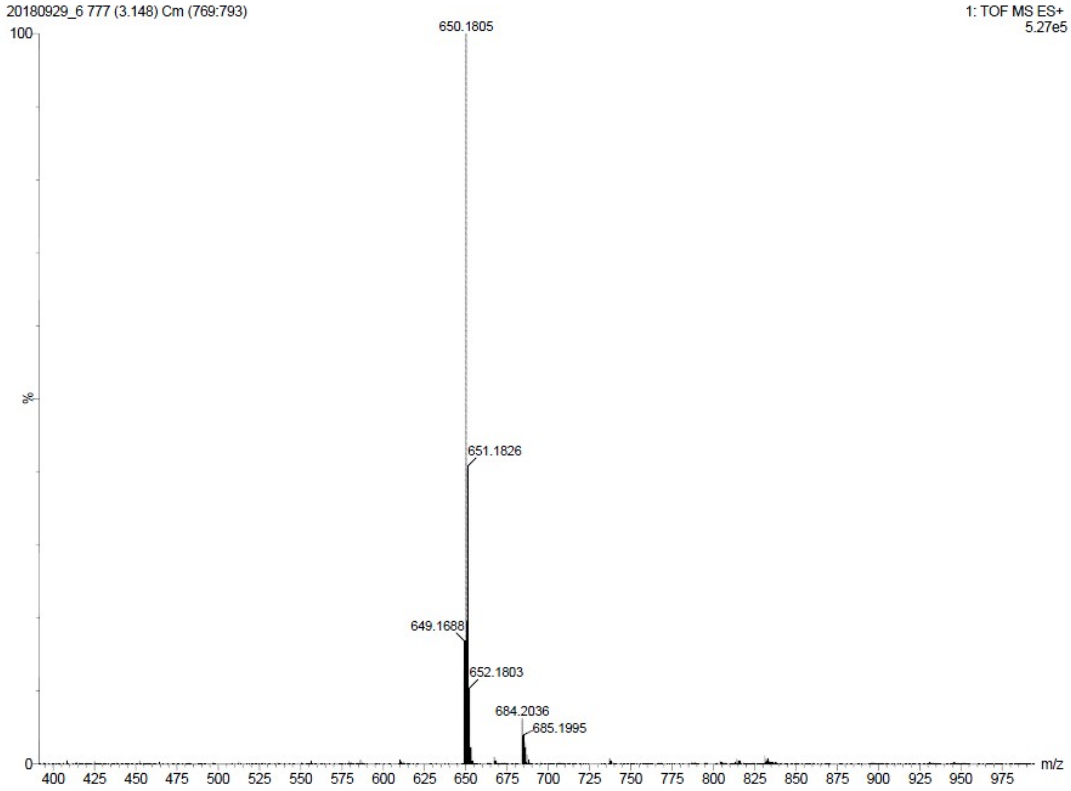

Fig. S22 The LC-MS of **$SFTO_2$-BzCz**

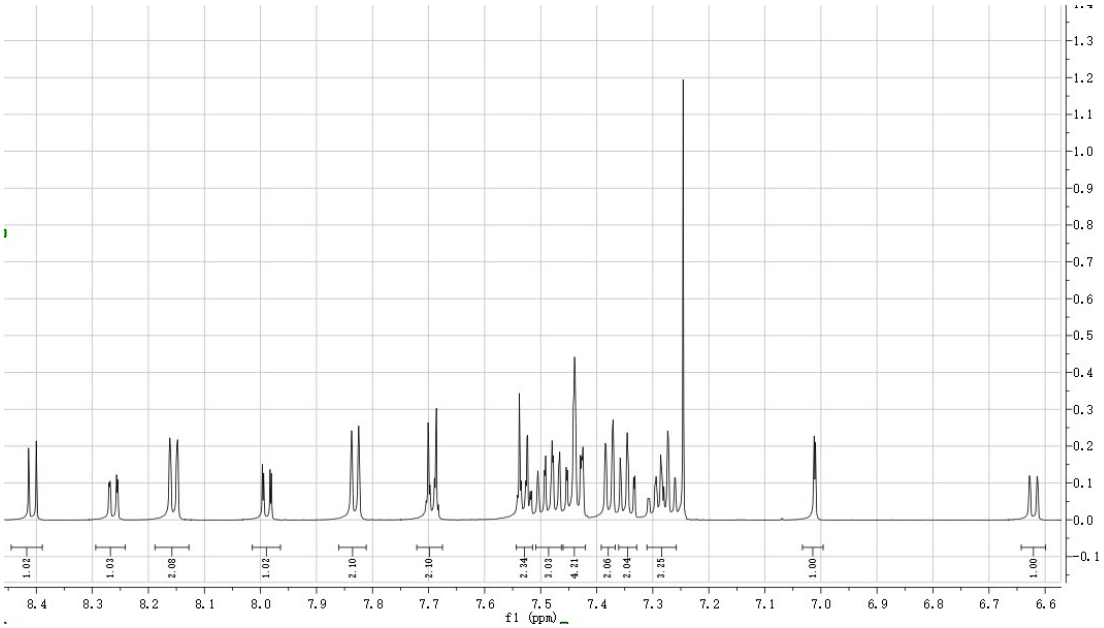

Fig. S23 ^{1}H NMR of **$SFTO_2$-BzCz** in $CDCl_3$

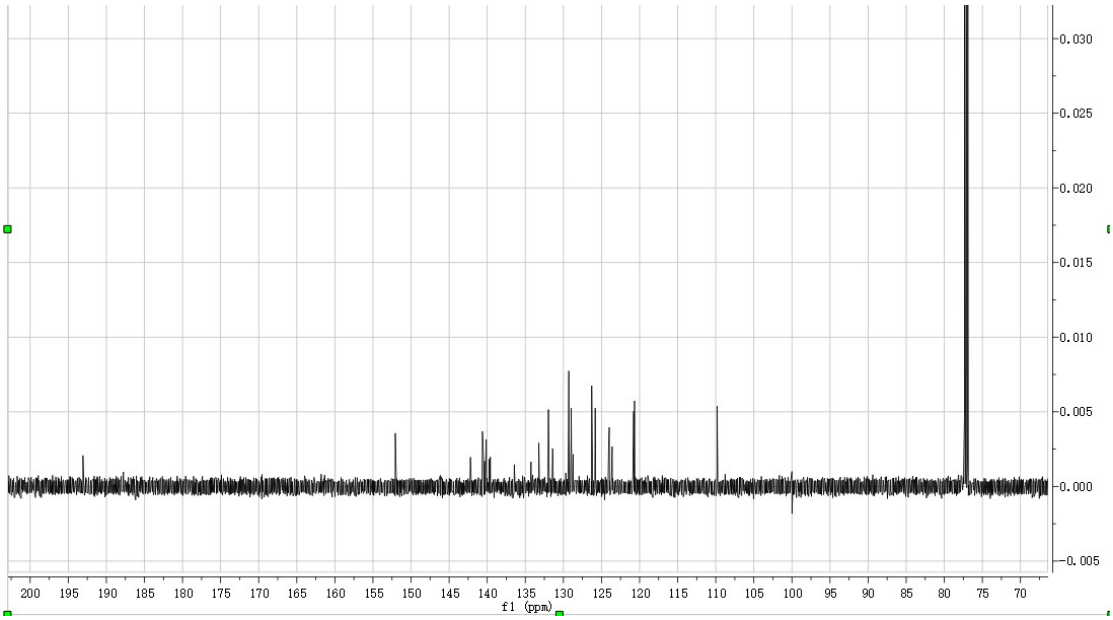

Fig. S24 ^{13}C NMR of **SFTO$_2$-BzCz** in $CDCl_3$